RSC Advances

ROYAL SOCIETY OF CHEMISTRY

www.rsc.org/advances

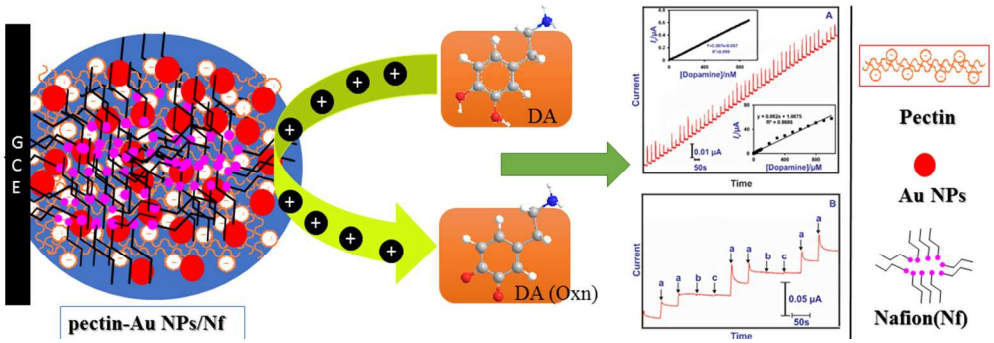

Electrodeposition of gold nanoparticles at pectin scaffold for selective determination of dopamine
304x101mm (96 x 96 DPI)

Electrodeposition of gold nanoparticles at pectin scaffold and its electrocatalytic application to the selective determination of dopamine

Rajkumar Devasenathipathy[a], Veerappan Mani[a], Shen-Ming Chen[a*], Balaji Viswanath[b], V.S. Vasantha[b*], Mani Govindasamy[c]

[a]Electroanalysis and Bioelectrochemistry Lab, Department of Chemical Engineering and Biotechnology, National Taipei University of Technology, No. 1, Section 3, Chung-Hsiao East Road, Taipei 106, Taiwan, ROC.

[b]Department of Natural Products Chemistry, Madurai Kamaraj University, Madurai, Tamil Nadu, India.

[c]Department of Chemistry, Bishop Heber College (Autonomous), Tiruchirappalli-620 017, Tamil Nadu, India.

Corresponding author, *Shen-Ming Chen: E-mail: smchen78@ms15.hinet.net. Tel: +886 2270 17147, Fax: +886 2270 25238.

Corresponding author, *V.S. Vasantha: E-mail: sivarunjan@gmail.com. Tel: + 91 - 452 - 245 8471, Ex: 108, Fax: + 91 - 452 - 245 8449.

Abstract

A simple electrochemical deposition strategy has been proposed for the preparation of gold nanoparticles (Au NPs) at the electrode surface using biopolymer pectin as stabilizing agent. The formation of the nanoparticles was confirmed by scanning electron microscopy (SEM), UV-Visible spectroscopy and X-ray diffraction (XRD) studies. Pectin stabilized gold nanoparticles film modified GCE (pectin-Au NPs/GCE) was prepared which exhibited excellent electrocatalytic ability towards oxidation of dopamine (DA). At the pectin-Au NPs/GCE, the redox couple corresponding to the redox reaction of DA was observed at the formal potential of 0.20 V with highly enhanced peak currents. A thin layer of nafion coating was applied on the pectin-Au NPs composite to improve the selectivity. Two linear ranges of detection were found: (1) 20 nM to 0.9 μM with LOD of 6.1 nM, (2) 0.9 μM to 1 mM with LOD of 0.64 μM. The fabricated sensor selectively detects DA even in the presence of high concentration of interferences. Moreover, the practical feasibility of the sensor has been addressed in pharmaceutical samples which present appreciable recovery results. The main advantages of sensor are very simple and green fabrication approach, roughed and stable, fast in sensing and highly reproducible sensor for dopamine.

Keywords: Electrodeposition, Pectin, gold nanoparticles, dopamine, selectivity, ascorbic acid.

1. Introduction

Over the past few decades, gold nanoparticles (Au NPs) have played significant role in nanoscience and nanotechnology due to its high stability, excellent electron conductivity and unique surface chemistry[1]. Specific size and morphology of the Au NPs have been the focus of intensive research because of its potential applications in the field of electronic, optical, optoelectronic and magnetic devices[2]. Till date, numerous methods such as chemical[3, 4], electrochemical[5, 6], irradiation[7] and microwave assisted methods[8, 9] have been employed for the synthesis of Au NPs. Among the aforementioned methods, electrochemical techniques are simple, eco-friendly, low cost and able to prepare uniform and size controllable nanoparticles[10]. In recent years, synthetic roots with novel protectors such as polymers, surfactants, ionic liquids and green agents have been designed for the synthesis of Au NPs to avoid nanoparticles agglomeration. Due to the excellent surface chemistry of Au NPs, they play a significant role in many scientific fields such as sensors[11], biosensors[12, 13], immunosensors[14], nanodevices[15] and biomedicines[16] etc.

Generally, capping reagents with functional group such as NH_2, COOH, SH and OH have explored for the synthesis of Au NPs[17]. In particular, green agents stabilized Au NPs have been intensified ascribed to their long-term stability, solubility, less toxicity and amphiphilicity. Functionalization with sugar polymers could be one of the facile ways to tailor the electronic and catalytic properties of the Au NPs[18]. Pectin (poly galacturonic acid) is a naturally occurring sugar polymer present at cell walls of plants is negatively charged, highly biocompatible, biodegradable, non-toxic and finds widespread applications in food, pharmaceutical and biomedical industries[19,20]. Remarkably, pectin contains –OH and –COOH functional groups which can be used to support the nanoparticles. However, till now only our reports available in the literature employing pectin as the stabilizing agent in Au NPs[21] and very few reports for chemical synthesis of other nanoparticles[21, 22].

Finding new approaches for the preparation of metal nanoparticles and exploring their electrochemical applications are continuous research interests in our research group[23, 24]. Recently, we have reported a fast microwave assisted chemical reduction method for the preparation of Au NPs on graphene nanosheets using polyethyleneimine as stabilizing agent[23]. However, this method requires microwave irradiation and reducing agent. In order to overcome these issues, herein we are reporting a

simple and green electrochemical deposition route for the preparation of gold nanoparticles at the electrode surface utilizing pectin as the scaffold and stabilizing agent (**scheme 1**).

Dopamine (DA) is one of the important catecholamine based neurotransmitter which transports signal from central nervous system to brain and plays vital role in the mammalian central nervous systems. Despites its valuable role in the biological function, abnormal concentration of DA resulting in brain disorders such as Parkinson's disease and schizophrenia[25-27] and therefore determination of DA is of great significance in the biological diagnoses. The electrochemical techniques are providing excellent platform for the detection of DA in biological diagnoses than the conventional methods due to its simplicity, selectivity, sensitivity and portability. However, the electrochemical signal of DA is often associated very close and overlaps with ascorbic acid (AA) and hence suffers from serious interference[28, 29]. Nevertheless, biological samples often contain high concentrations of AA than DA (100 to 1000 fold higher) and consequently overcoming the interference of AA is challenging task in the electrochemical determination of DA[29]. Several chemically modified electrodes have been employed in the literature in order to eliminate the interference from AA. In the present work, we prepared pectin stabilized Au NPs modified electrode for the selective determination of DA. A thin layer of nafion film was coated in order to eliminate the interference on AA. Therefore, the final sensor exhibits high electrocatalytic effect and the required selectivity even in the presence of high concentration of AA. We have compared the performance of our work with earlier Au NPs based electrochemical sensors; only two reports are showing similar limit of detection (LOD) for DA comparable to our work, however, none of the Au NPs sensors shows wide linear range of DA detection [23, 30, 31].

The main aim of the present work is to prepare highly stable Au NPs using pectin as scaffold and explore its electrocatalytic applications. The prepared nanoparticles are uniform, highly stable and exhibited excellent electrocatalytic ability towards determination of DA. The preparation of modified electrode is very fast (one step electrodeposition), green (does not involve any toxic reducing agents), simple electrode fabrication procedure, highly reproducible and stable.

2. Experimental

2.1 Reagents and apparatus

LM-pectin (DE 35%, genu pectin LM 12 CG-Z) and gold (III) chloride trihydrate (>99%, $HAuCl_4.3H_2O$), DA, AA and nafion (Nf) were purchased from Sigma-Aldrich and used as received. The supporting electrolyte used for all the electrochemical studies was 0.05 M Phosphate buffer solution (PBS), prepared using NaH_2PO_4 and Na_2HPO_4. The commercial sample of dopamine hydrochloride (easy dopa injection) was acquired from O-Smart Company, Taiwan (1.6 mg mL^{-1}, 8.44 mM) and diluted to the required concentrations in PBS (pH 7). Prior to each experiment, all the solutions were deoxygenated with pre-purified N_2 gas for 15 min unless otherwise specified.

The electrochemical measurements were carried out using CHI 611A electrochemical work station. Electrochemical studies were performed in a conventional three electrode cell using BAS glassy carbon electrode (GCE) as a working electrode (area= 0.071 cm^2), Ag|AgCl (saturated KCl) as a reference electrode and Pt wire as a counter electrode. Amperometric measurements were performed with analytical rotator AFMSRX (PINE instruments, USA) with a rotating disc electrode (RDE) having working area of 0.24 cm^2. Scanning electron microscope (SEM) studies were performed using Hitachi S-3000 H scanning electron microscope. Ultra violet visible (UV-Vis) spectroscopy studies were performed by U-3300 spectrophotometer. X-ray diffraction (XRD) studies were carried out using XPERT-PRO diffractometer using Cu Kα radiation (*k*=1.54 Å).

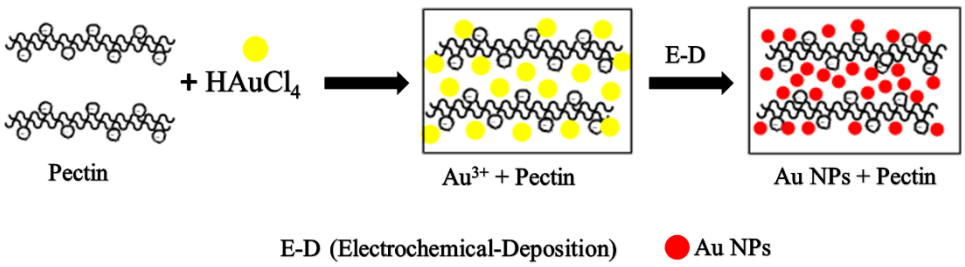

Scheme 1. Schematic representation for the preparation of pectin stabilized Au NPs

2.2 Electrodeposition of pectin stabilized Au NPs on GCE

GCE surface was polished with 0.05 µm alumina slurry using a Buehler polishing kit, then washed with water, ultrasonicated for 5 min and allowed to dry. After pre-cleaning, the GCE surface was transferred to the electrochemical cell to perform the electrodeposition of Au NPs. Ten consecutive

cyclic voltammograms (CVs) were swept at a scan rate of 25 mV s^{-1} between the potential ranges from + 1.40 V to –1.20 V in 0.1 M KNO_3 containing 3 mg/ml pectin and 0.3 mg/ml $HAuCl_4$. The as-prepared pectin stabilized Au NPs (pectin-Au NPs) modified electrode was rinsed with water and dried. Finally, 2 µL of 1.5% nafion (optimized concentration) was drop casted on the pectin-Au NPs/GCE and the resulting modified electrode has been denoted as GCE/pectin-Au NPs/Nf.

3. Results and Discussion

3.1. Characterization of pectin-Au NPs

Fig. 1A shows the electrochemical deposition of pectin-Au NPs in the potential range between 1.40 V to – 1.20 V. During the first scan, a large cathodic peak was observed at the potential of + 0.40 V corresponding to the reduction of Au^{3+} ions and nucleation of Au nanoparticles on the electrode surface. The evolution of hydrogen at the electrode surface is started at the potential of – 0.70 V and thereby generating the OH^- ions at the electrode-electrolyte interface. At this region, the cathodic electrodeposition of pectin has been taking place through the electrophoretic deposition. In the second cycle, the reduction peak current of Au NPs is doubled with shift in the reduction peak potential to 300 mV more positive side (+ 0.70 V) which indicating the growth of Au NPs. This catalytic behavior observed in the second cycle must be due to the deposition of Au NPs which is taking place on the pectin modified Au NPs/GCE surface not on the bare GC and thereby decreasing aggregation of gold nanoparticles. Hence, the interaction between –COOH and –OH with Au^{3+} ions may be leading to preconcentration of Au^{3+} ions in the electrode – electrolyte interface. In the reverse scan, a sharp anodic peak was observed at the potential of + 1.10 V should be ascribed to the oxidation of Au nanoparticles. During the continuous electrochemical cycling process, the growth of the reduction and oxidation peak currents reveals the successful formation of Au NPs[32]. The size and thickness of the pectin-Au NPs film have profound impact on the electrocatalytic efficiency which can be controlled by regulating scan rate and the number of cycles during electrodeposition. Therefore, we have optimized the number of cycles required to get optimum thickness of pectin-Au NPs film to give maximum electrocatalytic ability towards DA.

The electrocatalytic oxidation of DA (0.1 mM) was studied at pectin-Au NPs/GCE modified electrode by controlling the electrodeposition cycles from 1 to 12 in PBS (pH 7) at the scan rate of 0.05

Vs^{-1} (**Inset to Fig. 1A**). Since maximum electrocatalytic response of modified electrode for the oxidation of DA has been observed at 10 cycles of deposition, we have chosen 10 cycles of deposition as optimized cycles for further studies. Besides, the electrodeposition of Au NPs was taken without employing pectin scaffold (Fig. S1) as control. From this figure, we can see that the first and second cycles difference in cathodic peaks of the Au NPs is observed as 50 mV (but pectin-Au NPs is 300 mV) and anodic and cathodic peaks of Au NPs is saturated after 4 cycles. In order to evaluate the stability of the pectin-Au NPs/GCE, 200 successive CVs were recorded at pectin-Au NPs/GCE in PBS (pH 7) (Fig. S2). Only 8.3% of the initial peak currents were decreased even after 200 cycles which clearly revealing the excellent stability of the pectin-Au NPs/GCE. However, 14.3% of the initial peak currents were decreased after 200 consecutive scans at Au NPs/GCE (control) attributed to the instability of Au NPs formed without the aid of pectin scaffold which indicating the significant role of pectin in improving stability of the Au NPs.

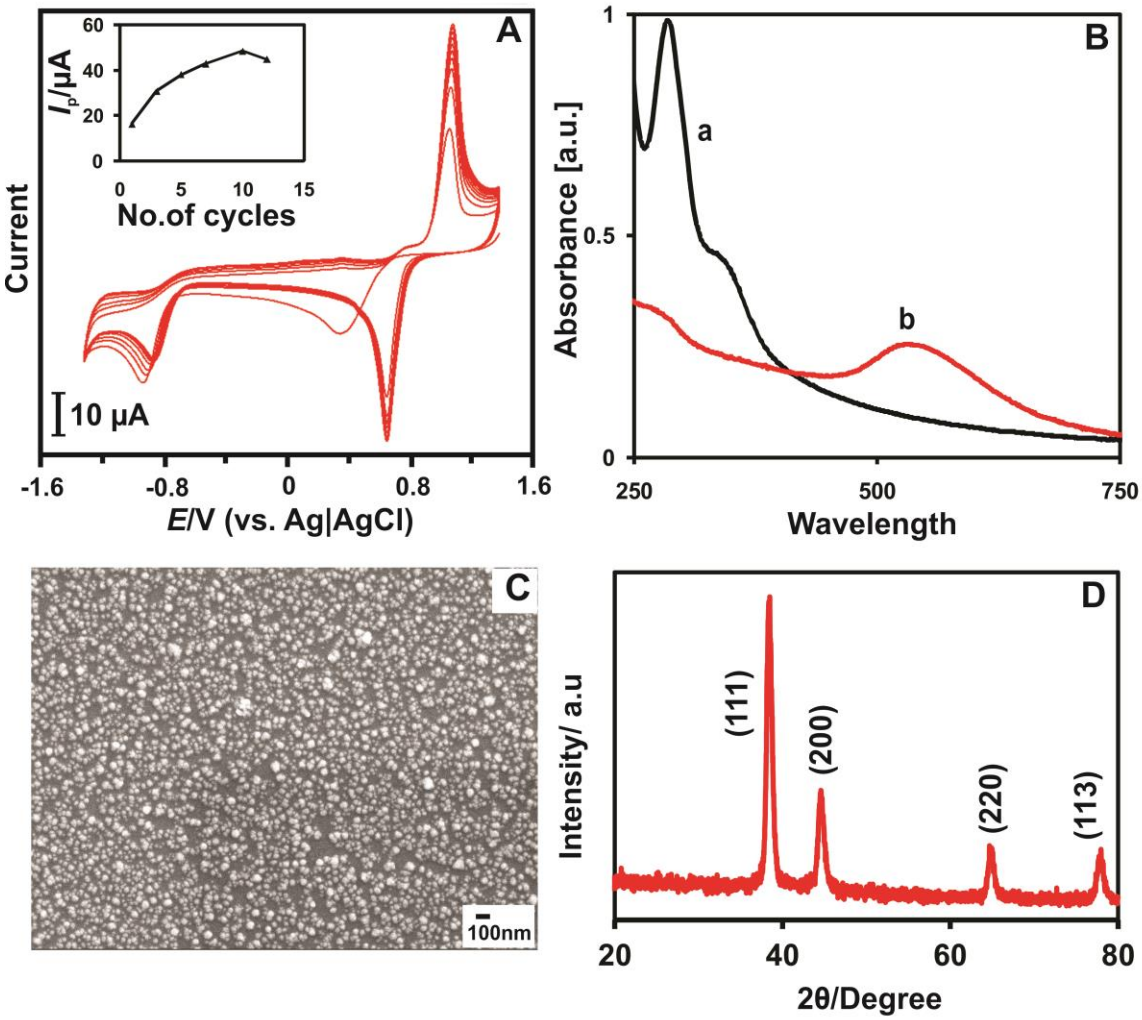

Fig. 1 (A) Electrochemical deposition of pectin stabilized Au nanoparticles in 0.1 M KNO_3 containing 3 mg/ml of pectin and 0.1 mM of $HAuCl_4$ at GCE for 10 cycles. Scan rate = 50 mV s^{-1}. (B) UV-Visible spectra of pectin (a) and pectin-Au NPs (b). (C) SEM image of Pectin-Au nanocomposite. (D) XRD pattern of pectin-Au NPs.

Fig. 1B displays the UV-Visible spectra of pectin (a) and pectin-Au NPs (b). The UV-Visible spectrum of pectin exhibited a sharp absorption peak at 290 nm and a broad shoulder peak at 380 nm that arose due to the free carboxyl group of pectin. However, these absorption peaks completely disappeared in the spectrum of pectin-Au NPs composite indicating that these free carboxyl groups were committed to accommodate Au NPs during electrochemical reduction. Meanwhile, the appearance of a new absorption peak at 560 nm revealed the successful formation of Au NPs[33]. The SEM image of pectin-Au NPs depicts the uniform decoration of Au nanoparticles onto the interconnected network of pectin scaffold (**Fig. 1C**). The Au NPs size is ranging from 15 to 40 nm validates the successful formation of Au NPs. However, the SEM image of Au NPs prepared without pectin exhibited the morphology of heavily aggregated Au NPs (Fig. S3). This result clearly revealing that the presence of pectin is necessary for the formation of stable Au NPs without aggregation. **Fig. 1D** displays XRD patterns of the pectin-Au NPs. The observation of four diffraction peaks at 2θ angles of 38.3°, 44.46°, 64.78° and 77.96° can be manifested to the (111), (200), (220) and (311) reflections of face-centered cubic structure of metallic Au NPs, respectively (JCPDS, card no. 04-0784)[34].

3.2 Electrocatalysis of DA at various modified electrodes

Fig. 2A shows the CVs obtained at unmodified (a), pectin-Au NPs(b), Au NPs/Nf (c) and pectin-Au NPs/ Nf (d) films modified GCEs in PBS (pH 7) at the scan rate of 25 mV s^{-1}. Electrochemical parameters of the redox reaction of DA at these modified electrodes such as, anodic peak current (I_{pa}) and cathodic peak current (I_{pc}), formal potential ($E^{o'}$) and peak potential separation value (ΔE_p) are given in **Table 1**.

Table 1: Electrochemical parameters for the redox reaction of DA at various modified electrodes

Electrode	E_{pa} **(V)**	E_{pc} **(V)**	$E^{o'}$**/V**	ΔE_p**/V**	I_{pa}**/μA**	I_{pc}**/μA**
Unmodified GCE	0.290	0.111	0.201	0.179	2.04	1.08

GCE/pectin-Au NPs	0.263	0.121	0.192	0.142	6.77	2.12
GCE/Au NPs/Nf	0.225	0.106	0.166	0.119	5.52	5.23
GCE/pectin-Au NPs/Nf	0.203	0.120	0.162	0.083	7.84	6.14

The electrocatalytic ability of these modified electrodes towards oxidation of DA are in the order of GCE/pectin-Au NPs/Nf/ > GCE/Au NPs/Nf > GCE/pectin-Au NPs > unmodified GCE. Among the above modified electrodes, GCE/pectin-Au NPs/Nf exhibited maximum electrocatalytic ability, whereas bare GCE exhibited poor electrocatalytic ability. Evidently, large ΔE_p value and high overpotential observed at the bare GCE revealed a sluggish electron transfer kinetic process for DA at this electrode. However, a pair of reversible redox peaks with highly enhance peak currents with very low ΔE_p have been observed at the pectin-Au NPs/Nf. Here, the anodic peak is attributed to the oxidation of DA to *o*-dopaminequinone, while the cathodic peak is due to the reduction of *o*-dopaminequinone back to DA[23]. Low ΔE_p and high peak currents observed at the GCE/pectin-Au NPs/Nf indicates the fast electron transfer kinetics and promising electrocatalytic ability of the modified electrode towards electrocatalysis of DA. Interestingly, Au NPs prepared without employing pectin scaffold have shown comparatively less electrocatalytic ability than that prepared with the aid of pectin as scaffold revealing that pectin act as excellent stabilizing agent and partially assist in the electrocatalysis of DA. Obviously, pectin acts as unique scaffold and stabilizing agent which provides excellent stability to the Au NPs which in turn provide stable electrocatalytic ability to catalyze DA. Au NPs prepared without pectin have shown poor stability caused by the aggregation of Au NPs which resulting in comparatively decreased electrocatalytic ability towards DA. Overall, the outstanding electrocatalytic ability of the GCE/pectin-Au NPs/Nf should be ascribed to the high surface area and high electrical conductivity of the Au NPs and also due to interactions between negatively charged functional groups present in the pectin and nafion film with positively charged DA.

Here, the purpose of employing thin layer of nafion coating is to block the electrochemical signal of AA, since Nf is a polymer that has the ability to hinder AA via electrostatic repulsive interaction between negatively charged Nf and negatively charged AA at pH 7[35-37]. However, Nf selectively allows the movement of DA through attractive electrostatic interaction between negatively charged Nf and positively charged DA. Also, we optimized the concentration of Nf which required to prohibit the interference of maximum amount of AA (**Fig. S4A**). We found that upon increasing the percentage concentration of Nf from 1% to 1.5%, the response current for DA increases and become stable at 1.5%.

Therefore we used that concentration as optimized concentration of Nf to make a thin layer coating on the pectin-Au NPs modified GCE.

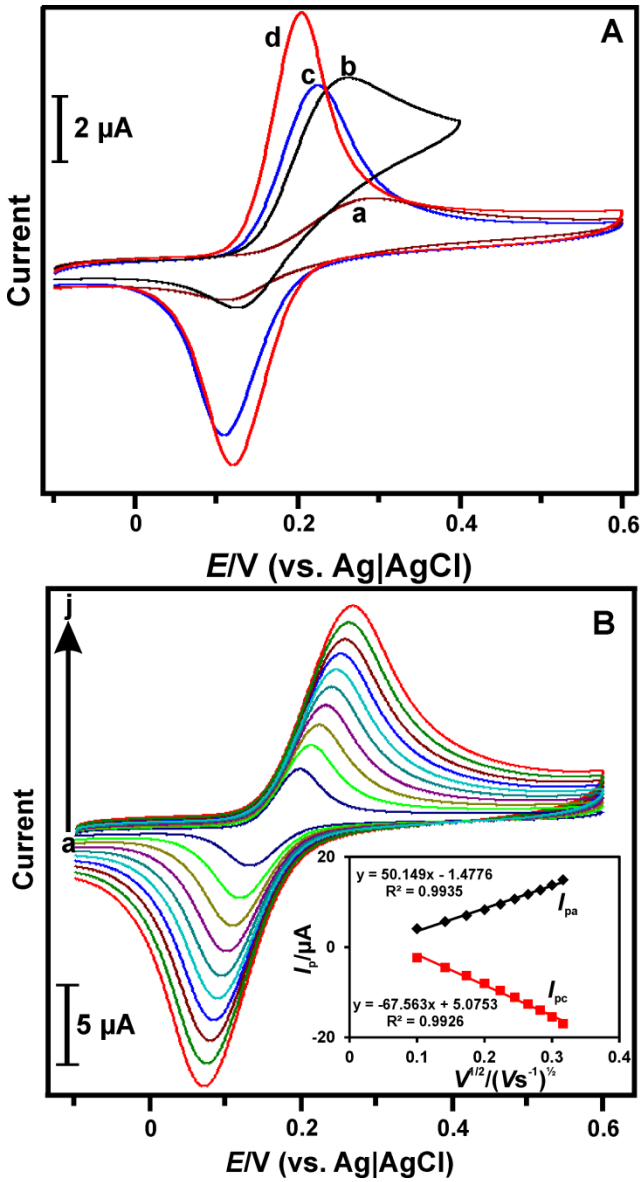

Fig. 2 (A) CVs obtained at unmodified (a), pectin-Au NPs(b), Nf/Au NPs (c) and pectin-Au NPs/Nf (d) films modified GCEs in PBS (pH 7) containing 0.1 mM DA at the scan rate of 25 mVs^{-1}. (B) CVs obtained at GCE/pectin-Au NPs/Nf in PBS (pH 7) containing 0.1 mM DA at different scan rates from 0.01 Vs^{-1} to 0.1Vs^{-1}. Inset: Plot of $v^{1/2}$ vs. I_p.

We have studied the oxidation of AA for different concentrations at GCE/pectin-Au NPs/Nf (**Fig. S4B**). Upon addition of AA from 1 mM to 5 mM, only background current was increased, whereas no obvious response currents were observed for AA. The percent interferences of each concentrations of

AA at the GCE/pectin-Au NPs/Nf have been calculated in terms of changes in the signal ratio to the blank signal and presented as Table S1 which shows negligible interference of AA (less than 5%). **Fig. S4C** shows comparison between the electrocatalytic response of GCE/pectin-Au NPs/Nf towards oxidation of 2 mM AA and 0.5 mM AA. As can be seen from the figure, GCE/pectin-Au NPs/Nf exhibited highly enhanced peak currents to the oxidation of DA, whereas it did not show obvious peak for the addition of AA. Thus, the Nf coating acts as gateway at the pectin-Au NPs electrode surface by permitting DA and preventing major portion of AA to reach the electrode surface.

The effect of scan rate (v) towards redox reaction of DA at the GCE/pectin-Au NPs/Nf has been investigated in PBS (pH 7) containing 0.1 mM DA at the scan rate (v) ranges from 0.01 to 0.1 Vs^{-1} (**Fig. 2B**). Both I_{pa} and I_{pc} increases as scan rate increases from 0.01 to 0.1 Vs^{-1}. Upon scan rate increases, I_{pa} shifted to positive potential side, whereas I_{pc} shifted to negative potential side. Moreover, a plot of square root of scan rates ($v^{1/2}$) versus I_{pa} and I_{pc} exhibited linear relationship indicating that the redox behavior of DA at GCE/pectin-Au NPs/Nf is controlled by diffusion (**inset to Fig. 2B**). The corresponding linear regression equation can be expressed as: I_{pa} (μA) = 50.15 $v^{1/2}$ $(Vs^{-1})^{1/2}$ – 1.48, R^2 = 0.993 and I_{pc} (μA) = -67.56 $v^{1/2}$ $(Vs^{-1})^{1/2}$ + 5.07, R^2 = 0.993.

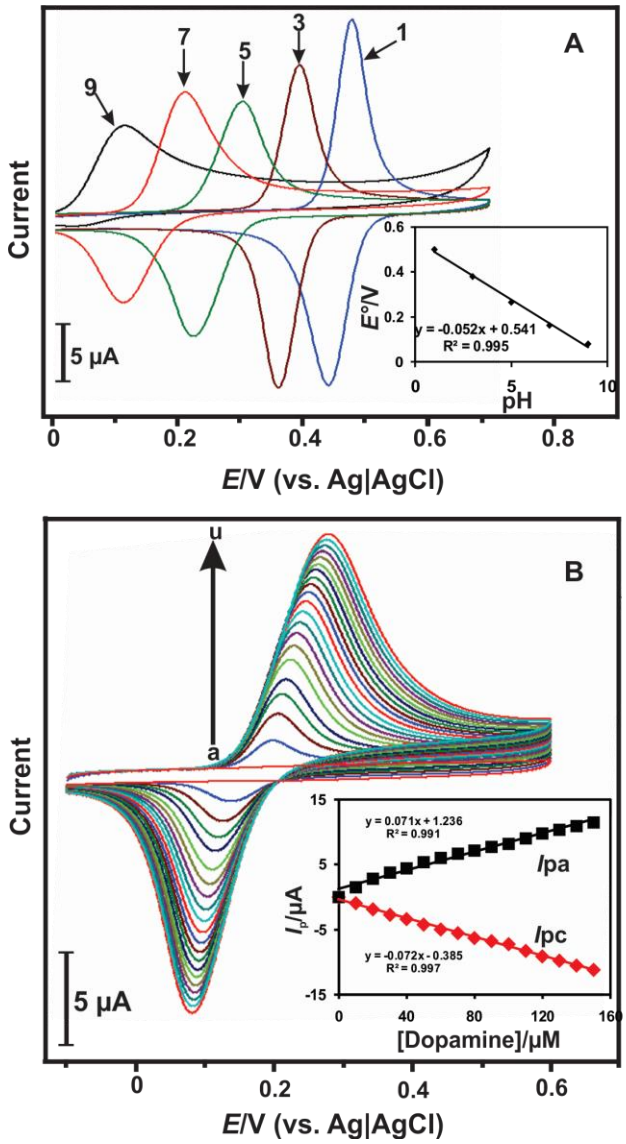

Fig. 3 (A) CVs obtained at GCE/pectin-Au NPs/Nf in PBS of various pH solutions (pH 1–9) in the presence of 0.1 mM DA at the scan rate of 25 mV s^{-1}. Inset: Plot of E^{o}/V vs. pH.(B) CVs obtained at GCE/pectin-Au NPs/Nf in the absence (a) and presence of DA from 10 μM to 200 μM (curves b to u; each 10 μM addition) in PBS (pH 7) at the scan rate 25mVs^{-1}. Inset: Plot of I_p vs. [DA].

3.3 pH studies

In the **fig. 3A** shows the various pH of the supporting electrolyte towards redox peaks of DA at the GCE/pectin-Au NPs/Nf was investigated in PBS (pH 7) containing 0.1 mM of DA. Both E_{pa} and E_{pc} of the redox peak were shifted towards the negative direction of the potential upon increasing pH from 1 to 9 indicating that the redox reaction of DA occurring at this modified electrode is pH dependent. A

plot of $E^{0'}$ of the redox peaks of DA versus various pH rendered linear plot with slope value of −52.0 mV/pH. The slope value is found to be in close agreement with the theoretical value of −59 mV/pH at 25 °C for a reversible electron transfer reaction involves transfer of equal numbers of protons and electrons[38].

3.4 Electro-oxidation of DA

Fig. 3B shows the CVs obtained at GCE/pectin-Au NPs/Nf in the absence (curve a) and presence of DA (curves b to u; each addition of 10 µM) in PBS (pH 7). Upon addition of 10 µM DA into the PBS solution, an obvious redox peaks are observed; further, the peak current increases linearly upon additions of DA from 10 to 200 µM. The linear increase in the I_{pa} and I_{pc} reveals the occurrence of efficient electrocatalytic ability of the electrode without any fouling effect. A plot of I_{pa} and I_{pc} versus concentration of DA exhibited linear relationship (**inset to Fig.3B**) with linear concentration range of 10 – 200 µM.

3.5 Rotating disc electrode studies

The electrocatalytic activity of pectin-Au NPs/Nf modified electrode towards oxidation of DA was evaluated by rotating disc electrode (RDE) experiments. **Fig. 4A** shows the current–potential curves at the GCE/pectin-Au NPs/Nf in PBS (pH 7) in the absence (a) and presence of DA (each 50 µM addition, from b to k). Well defined voltammograms with mass transport limited current were observed upon each addition. The disc current (I_d) increases linearly with the increase in concentration of DA. A plot between I_d and concentration of DA exibited a linear relationship with slope 0.148 µA µM^{-1} **(Inset to Fig. 4A)**.

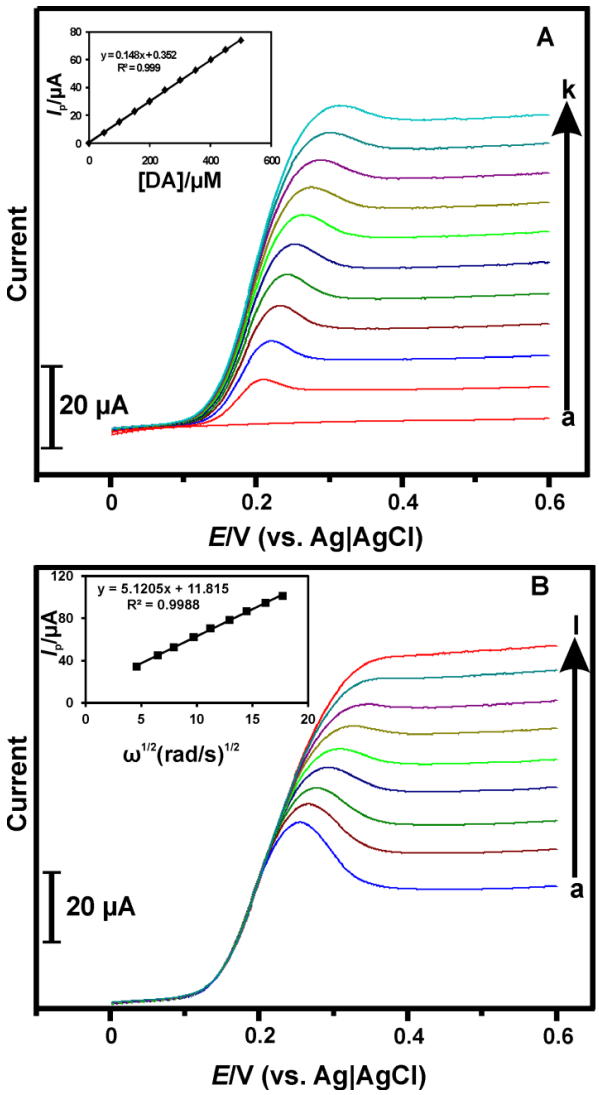

Fig. 4 (A) RDE voltammograms obtained at the GCE/pectin-Au NPs/Nf in the absence of DA (a) and presence of each 50 μM addition of DA (b-k) in PBS (pH 7) at the rotation speed of 1500 RPM. (B) RDE voltammograms of GCE/pectin-Au NPs/Nf in the presence of 0.5 mM DA at different rotation rates (a) 200, (b) 400, (c) 600, (d) 900, (e) 1200, (f) 1600 (h) 2500 and 3000 RPM.

Fig. 4B presents the current–potential curves at RDE/pectin-Au NPs/Nf for different rotation rates such as (a) 200, (b) 400, (c) 600, (d) 900, (e) 1200, (f) 1600 (h) 2500 and 3000 RPM in (PBS (pH 7) containing 0.5 mM DA. Levich plot was drawn from the data obtained from RDE voltammograms and given as **inset to Fig. 5B.** The Levich plot is found to be linear which indicating that the oxidation of DA at RDE/pectin-Au NPs/Nf is mass transport-limited. The relationship between the limiting current and rotating speed of the electrode can be realted by Levich equation (1)[39].

$$I_L = I_{LEV} = 0.620\, nFAD_0^{2/3}\gamma^{-1/6}\omega^{1/2}C_0 \quad (1)$$

Where, D_0, γ, ω and C_0 are the diffusion co-efficient, kinematic viscosity, rotation speed and bulk concentration of the reactant in the solution, respectively. The remaining parameters in the equation stands for their conventional meanings. By substituting all the values in the above equation (1), the value of D_0 is calculated to be about 5.71×10^{-6} $cm^2\ s^{-1}$ which is quite comparable with the values obtained by the previous reports for the electrocatalysis of DA[40].

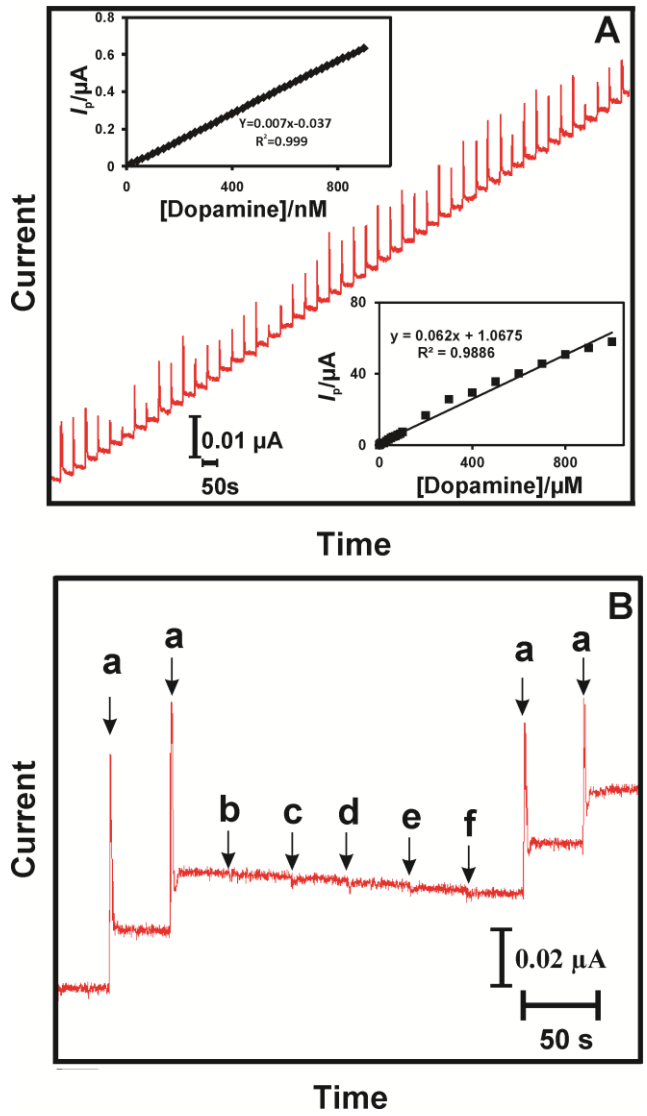

Fig. 5 (A) Amperometric i-t response obtained at pectin-Au NPs/Nf film modified rotating disc GCE upon each addition of 20 nM DA into continuously stirred PBS (pH 7) at the rotation speed of 1500 RPM. E_{app} = + 0.20 V. Inset (a) and (b): Plot of [DA] vs. I_p. (B). Amperometric response of pectin-Au

NPs/Nf film modified rotating disc GCE for the 100 nM addition of DA (a) in the presence of 2 mM of AA (b), uric acid (c) arterenol (d), histidine (e) and tyrosine (f).

3.6 Amperometric determination of DA

Fig. 5A shows the amperometric i-t response of pectin-Au NPs/Nf film modified rotating disc GCE upon sequential injection of 20 nM DA into PBS (pH 7) at regular interval of 50s into continuously stirred PBS (pH 7) at the rotation speed of 1500 RPM. The applied potential (E_{app}) of the electrode was hold at + 0.20 V. For every addition of DA, quick and stable amperometric responses were observed. The amperometric response current reaches its 95% steady-state current within 5s indicating fast electrocatalytic oxidation of DA at the GCE/pectin-Au NPs/Nf. A plot between concentration of DA and peak current exhibited linear relationship and sensor working linear range was found to be between 20 nM and 0.9 µM **(Insets a, Fig. 5A).** The respective linear regression equation expressed as I_p/µA =0.007 [DA]/µAnM^{-1}– 0.037; R^2=0.99. Sensitivity of the sensor is calculated to be 0.033 µAnM^{-1} cm^{-2} and low limit of detection (LOD) is calculated to be 6.1 nM. The LOD of the sensor was calculated by using the formula, LOD= 3 s_b/S (where, s_b =standard deviation of blank signal and S =sensitivity)[41]. A second linear range was observed in the higher concentration of DA between 0.9 µM and 1 mM **(Insets b, Fig. 5A)** and the respective linear regression equation was expressed as: I_p/µA =0.062[DA]/µAµM^{-1} + 1.067 (± 1.23); R^2 = 0.986.The sensitivity and LOD at this linear range was calculated to be 0.2952 µAµM^{-1} cm^{-2} and 0.64 µM, respectively. The analytical performance of the proposed sensor towards determination of DA is superior over the other reports in terms of wide linear ranges, high sensitivity and low LOD (**Table 2**).

Table 2: Comparison of analytical parameters for the determination of DA at GCE/pectin-Au NPs/Nf nanocomposite film modified electrode with other films modified electrodes

Electrode	Linear range/µM	Limit of detection/µM	Sensitivity	Ref.
Au NPs@SiO2– molecularly imprinted polymers	0.048–5	0.02	–	25
graphene/polyethylene	2–48	0.13	2.635 µAµM^{-1} cm^{-2}	23

imine/Au NPs				
Fe3O4@ molecularly imprinted polymers/GS-chitosan	0.5-500	0.02	–	[30]
gold nanoparticles coated polystyrene/reduced graphite oxide microspheres	0.05–20	5×10^{-3}	3.44 $\mu A \mu M^{-1} cm^{-2}$	[42]
Au@ carbon dots–chitosan composite	0.01–100.0	1×10^{-3}	–	[31]
graphene sheets and Au NPs modified carbon fiber electrode	0.59–43.96	0.59	–	[43]
pectin-Au NPs/Nf	0.02–0.9; 0.9–1000	6.1×10^{-3}; 0.64	0.033 $\mu A n M^{-1} cm^{-2}$ 0.2952 $\mu A \mu M^{-1} cm^{-2}$	This work

The selectivity of the pectin-Au NPs/Nf modified electrode to detect DA in the presence of common interferences was investigated (**Figure 5 B**). The operating potential of the electrode was hold at + 0.20 V, while the rotation speed was kept at 1500 RPM. The modified electrode exhibited well defined amperometric response to the addition of 100 nM DA, whereas no recognizable responses were observed for the addition of 2 mM AA (b), uric acid (c), arterenol (d), histidine (e) and tyrosine (f). However, notable amperometric response was observed for the addition of 100 nM DA into the same PBS solution containing all the aforementioned interferences. Therefore, pectin-Au NPs/Nf film modified electrode has the ability to selectively access DA even in the presence of 5000 fold excess concentration of AA, uric acid, arterenol, histidine and tyrosine revealing the outstanding selectivity of the modified electrode. As explained in the previous section, electrostatic repulsion between negatively charged modified electrode surface and negatively charged aforementioned interferences assisted to repel and eliminate the interferences.

3.7 Stability, repeatability and reproducibility studies

In order to determine storage stability of the modified electrode, the electrocatalytic response of the GCE/pectin-Au NPs/Nf towards 0.1 mM DA was monitored every day. The electrode was kept stored in PBS (pH 7) at 4°C when not in use. During one month storage period, the fabricated sensor presented well defined catalytic response without any shift in the peak potential. Moreover, 93.15% of the initial I_{pa} was retained over one month of its continuous use, revealing the good storage stability of the sensor. Furthermore, the operational stability of the modified electrode was investigated upon continuous rotation of the pectin-Au NPs/Nf modified GCE at the rotation speed of 1500 rpm in PBS (pH 7). Stable amperomerometric response was observed for the addition of 100 nM of DA. Only 7.2% of the initial response current is decreased even after continously rotated for 3500 s revealing the good operational stability of the modified electrode. Repeatability and reproducibility of the proposed sensor was evaluated in PBS (pH 7) containing 0.1 mM DA at the scan rate of 25 mVs^{-1}. The sensor exhibits appreciable repeatability with relative standard deviation (R.S.D) of 2.08% for 10 repeatitive measurements carried out using single electrode. In addition, the sensor exhibits promising reproducibility of 1.92% for the five independent measurments carried out in five different electrodes.

3.8 Real sample

The practical feasibility of the sensor was assessed in commercial acquired dopamine hydrochloride injection sample (8.44 mM). The concentration of the injection sample has been diluted to the final concentrations of 1 µM and 100 nM. The amperometric experiments were performed using GCE/pectin-Au NPs/Nf by following the optimized experimental conditions used for the analysis of lab samples. The results are presented as Table 3. The appreciable found and recovery results revealing that pectin-Au NPs/Nf modified GCE exhibited promising practical feasibility to determine the concentration of DA present in real samples.

Table 3. Determination of DA present in pharmaceutical samples using GCE/pectin-Au NPs/Nf.

Real Sample	Sample	Concentration samples (added)	Found	Recovery	RSD
Dopamine hydrochloride injection	1	100 nM	98.2 nM	98.2	3.1
	2	1 µM	0.98 µM	98	2.4

4. Conclusions

We have described a simple electrochemical deposition strategy for the preparation of Au NPs using pectin as a stabilizing agent. The pectin backbone acts as versatile scaffold for the formation of highly decorated Au NPs. The successful formation of the nanoparticles was confirmed by CV, SEM, UV-Visible spectroscopy and XRD studies. GCE/pectin-Au NPs/Nf exhibited excellent electrocatalytic ability towards determination of DA. The amperometric sensor presented excellent analytical parameters towards detection of DA. Two linear ranges were found: (1) from 20 nM to 0.9 μM with LOD of 6.1 nM, while second linear was observed between 0.9 μM to 1 mM with LOD of 0.64 μM. The sensor has exhibited high selectively and shown promising practical feasibility in pharmaceutical samples.

Acknowledgement

This work was supported by the National Science Council and the Ministry of Education of Taiwan (Republic of China).

References

1. J. Shan and H. Tenhu, *Chem. Commun.*, 2007, 4580-4598.
2. J. Zhang, J. Du, B. Han, Z. Liu, T. Jiang and Z. Zhang, *Angew. Chem. Int. Ed.*, 2006, **118**, 1134-1137.
3. B. K. Jena and C. R. Raj, *Langmuir*, 2007, **23**, 4064-4070.
4. Y. Shao, Y. Jin and S. Dong, *Chem. Commun.*, 2004, 1104-1105.
5. L. Wang, W. Mao, D. Ni, J. Di, Y. Wu and Y. Tu, *Electrochem. Commun.*, 2008, **10**, 673-676.
6. M. -H. Xue, Q. Xu, M. Zhou and J.-J. Zhu, *Electrochem. Commun.*, 2006, **8**, 1468-1474.
7. K. Mallick, Z. Wang and T. Pal, *J. Photochem. Photobiol., B*, 2001, **140**, 75-80.
8. C. G.-Wing, R. Esparza, C. V.-Hernandez, M. F. Garcia and M. J.-Yacaman, *Nanoscale*, 2012, **4**, 2281-2287.
9. N. Arshi, F. Ahmed, S. Kumar, M. Anwar, J. Lu, B. H. Koo and C. G. Lee, *Curr. Appl. Phys.*, 2011, **11**, S360-S363.
10. X. -L. Luo, J. -J. Xu, Y. Du and H. -Y. Chen, *Anal. Biochem.*, 2004, **334**, 284-289.
11. D. D. Liana, B. Raguse, L. Wieczorek, G. R. Baxter, K. Chuah, J. J. Gooding and E. Chow, *RSC Adv.*, 2013, **3**, 8683-8691.
12. O. Shulga and J. R. Kirchhoff, *Electrochem. Commun.*, 2007, **9**, 935-940.
13. J. M. Pingarrón, P. Y. -Sedeño and A. G. -Cortés, *Electrochim. Acta*, 2008, **53**, 5848-5866.
14. B. S. Munge, C. E. Krause, R. Malhotra, V. Patel, J. S. Gutkind and J. F. Rusling, *Electrochem. Commun.*, 2009, **11**, 1009-1012.
15. D. A. Zweifel and A. Wei, *Chem. Mater.*, 2005, **17**, 4256-4261.
16. E. C. Dreaden, A. M. Alkilany, X. Huang, C. J. Murphy and M. A. El-Sayed, *Chem. Soc. Rev.*, 2012, **41**, 2740-2779.
17. X. Lü, Y. Song, A. Zhu, F. Wu and Y. Song, *Int. J. Electrochem. Sci*, 2012, **7**, 11236-11245.
18. S. Guo and E. Wang, *Anal. Chim. Acta*, 2007, **598**, 181-192.
19. N. Zakharova, K. Kydralieva, E. Khudaibergenova, N. Gorbunova, S. Pomogailo, G. I. Dzhardimalieva, A. Pomogailo and S. Jorobekova, *Makromol. Chem. Macromol. Symp.*, 2012.
20. H. Jonassen, A. Treves, A.-L. Kjøniksen, G. Smistad and M. Hiorth, *Biomacromol.*, 2013, **14**, 3523-3531.
21. A. Khazaei, S. Rahmati, Z. Hekmatian and S. Saeednia, *J. Mol. Cat. A: Chem.*, 2013, **372**, 160-166.

22. F.-T. J. Ngenefeme, N. J. Eko, Y. D. Mbom, N. D. Tantoh and K. W. Rui, *Open J. Comp. Mat.*, 2013, **3**, 30.
23. V. K. Ponnusamy, V. Mani, S. -M. Chen, W. -T. Huang and J. Jen, *Talanta*, 2014, **120**, 148-157.
24. R. Devasenathipathy, V. Mani, S. -M. Chen, D. Arulraj and V. Vasantha, *Electrochim. Acta*, 2014, **135**, 260-269.
25. D. Yu, Y. Zeng, Y. Qi, T. Zhou and G. Shi, *Biosens. Bioelectron.*, 2012, **38**, 270-277.
26. C. Xue, Q. Han, Y. Wang, J. Wu, T. Wen, R. Wang, J. Hong, X. Zhou and H. Jiang, *Biosens. Bioelectron.*, 2013, **49**, 199-203.
27. Z. Wang, J. Liu, Q. Liang, Y.Wang and G. Luo, *Analyst*, 2002, **127**, 653-658
28. D. Wu, H. Li, X. Xue, H. Fan, Q. Xin and Q. Wei, *Anal. Methods*, 2013, **5**, 1469-1473.
29. B. Liu, H. T. Lian, J. F. Yin and X. Y. Sun, *Electrochim. Acta*, 2012, **75**, 108-114.
30. M. Liu, Q. Chen, C. Lai, Y. Zhang, J. Deng, H. Li and S. Yao, *Biosens. Bioelectron.*, 2013, **48**, 75-81.
31. Q. Huang, H. Zhang, S. Hu, F. Li, W. Weng, J. Chen, Q. Wang, Y. He, W. Zhang and X. Bao, *Biosens. Bioelectron.*, 2014, **52**, 277-280.
32. M. Rajkumar, S. -C. Chiou, S. -M. Chen and S. Thiagarajan, *Int. J. Electrochem. Sci*, 2011, **6**, 3789-3800.
33. Y. Li, T. -Y. Wu, S. -M. Chen, M. A. Ali and F. M. AlHemaid, *Int. J. Electrochem. Sci*, 2012, **7**, 12742-12751.
34. J. Heo, D. -S. Kim, Z. H. Kim, Y. W. Lee, D. Kim, M. Kim, K. Kwon, H. J. Park, W. S. Yun and S. W. Han, *Chem. Commun.*, 2008, 6120-6122.
35. R. Thangamuthu, Y. C. Wu and S. M. Chen, *Electroanalysis*, 2009, **21**, 994-998.
36. S. Yang, G. Li, Y. Yin, R. Yang, J. Li and L. Qu, *J. Electroanal. Chem.*, 2013, **703**, 45-51.
37. E. Canbay and E. Akyilmaz, *Anal. Biochem.*, 2014, **444**, 8-15.
38. V. Mani, B. Devadas and S. -M. Chen, *Biosens. Bioelectron.*, 2013, **41**, 309-315.
39. C. R. Raj, T. Okajima and T. Ohsaka, *J. Electroanal. Chem.*, 2003, **543**, 127-133.
40. V. Vasantha and S. -M. Chen, *J. Electroanal. Chem.*, 2006, **592**, 77-87.
41. A. Radoi and D. Compagnone, *Bioelectrochemistry*, 2009, **76**, 126-134.
42. T. Qian, C. Yu, S. Wu and J. Shen, *Colloids Surf., B*, 2013, **112**, 310-314.
43. J. Du, R. Yue, F. Ren, Z. Yao, F. Jiang, P. Yang and Y. Du, *Gold Bull.*, 2013, **46**, 137-144.